(s being the value of r on the surface S) the surface integral in eq A1 vanishes.

B. Leibnitz Rule. The quantity

$$\int_V (\partial u/\partial t) \exp(-i\beta\cdot\mathbf{r})\, d\mathbf{r}$$

can be transformed into

$$\frac{d}{dt}\int_V u \exp(-i\beta\cdot\mathbf{r})\, d\mathbf{r} - \int_S u\mathbf{V}_s \exp(-i\beta\cdot\mathbf{r})\, d\mathbf{S}$$

by the application of the Leibnitz rule.[37] In the second integral, $\mathbf{V}_s$ denotes the normal velocity of the surface. With the above-mentioned periodic boundary conditions (eq A4), the surface integral vanishes.

References and Notes

(1) Broens, L.; Altena, F. W.; Smolders, C. A.; Koenhen, D. M. *Desalination* **1980**, *32*, 33.
(2) Volmer, M.; Weber, A. *Z. Phys. Chem.* **1925**, *119*, 277.
(3) Cahn, J. W. *Acta Metall.* **1961**, *9*, 795.
(4) Flory, P. J. *J. Chem. Phys.* **1942**, *10*, 51.
(5) Huggins, M. L., presented before the Wilder D. Bancroft Colloid Symposium, Ithaca, New York, June 20, 1941.
(6) Flory, P. J. Fifteenth Spiers Memorial Lecture, *Trans. Faraday Soc.* **1970**.
(7) Flory, P. J.; Eichinger, B. E. *Trans. Faraday Soc.* **1968**, *64*, 2035.
(8) Flory, P. J.; Hoeker, H. *Trans. Faraday Soc.* **1971**, *67*, 2258.
(9) Prigogine, I.; Bellemans, A.; Mathot, V. "The Molecular Theory of Solutions"; North Holland: Amsterdam, 1957; Chapter 16.
(10) Patterson, D. *Macromolecules* **1969**, *2*, 672.
(11) Heil, J. F.; Prausnitz, J. M. *AIChE J.* **1969**, *12*, 678.
(12) Bonner, D. C.; Prausnitz, J. M. *AIChE J.* **1973**, *19*, 943.
(13) Renuncio, J. A. R.; Prausnitz, J. M. *Macromolecules* **1976**, *9*, 898.
(14) McMaster, L. P. "Aspects of Liquid–Liquid Phase Transition Phenomena in Multicomponent Polymeric Systems"; Platzer, N. B., Ed.; American Chemical Society: Washington, DC, 1975; Adv. Chem. Ser., No. 142, pp 43–65.
(15) Nishi, T.; Wang, T. T., Kwei, T. K. *Macromolecules* **1975**, *8*, 227.
(16) Cahn, J. W.; Hilliard, J. E. *J. Chem. Phys.* **1958**, *28*, 258.
(17) Rao, M.; Kalos, M. H.; Lebowitz, J. L.; Marro, J. *Phys. Rev. B: Solid State* **1976**, *13*, 4328.
(18) Bortz, A. B.; Kalos, M. H.; Lebowitz, J. L.; Zendejas, M. A. *Phys. Rev. B: Solid State* **1974**, *10*, 535.
(19) Levy, A.; Reich, S.; Meakin, P. *Phys. Lett. A* **1982**, *87A*, 248.
(20) Sanji, P. S.; Gunton, J. D.; Katz, S. L.; Timpe, R. H. *Phys. Rev. B: Condens. Matter* **1982**, *25*, 389.
(21) Kock, S. W.; Desai, R.; Abraham, F. F. *Phys. Rev. A* **1982**, *26*, 1015.
(22) Haus, J. W.; King, H. *Phys. Rev. B: Condens. Matter* **1982**, *2*, 3298.
(23) Abraham, F. F.; Schreiber, D. E.; Mruzik, M. R.; Pound, G. M. *Phys. Rev. Lett.* **1976**, *36*, 261.
(24) Mruzik, M. R.; Abraham, F. F.; Pound, G. M. *J. Chem. Phys.* **1978**, *69*, 3462.
(25) Vrentas, J. S.; Duda, J. L. *J. Polym. Sci., Polym. Phys. Ed.* **1977**, *15*, 403.
(26) Vrentas, J. S.; Duda, J. L. *J. Polym. Sci., Polym. Phys. Ed.* **1977**, *15*, 417.
(27) Vrentas, J. S.; Duda, J. L. *Macromolecules* **1976**, *9*, 785.
(28) Vrentas, J. S.; Duda, J. L.; Ni, L. W. *Macromolecules* **1983**, *16*, 261.
(29) de Fontaine, D. Ph.D. Dissertation, Northwestern University, Evanston, IL, 1967.
(30) Tompa, H. "Polymer Solutions"; Butterworths: London, 1956.
(31) Smolders, C. A.; van Aartsen, J. J.; Steenbergen, A. *Kolloid Z. Z. Polym.* **1971**, *243*, 14.
(32) de Fontaine, D. "Thermodynamics and Kinetics of Phase Separation, Metallurgical Treatises"; Tien, J. K.; Elliott, J. F., Ed.; American Institute of Metallurgical Engineers: Warrendale, PA, 1981; pp 423–444.
(33) Feke, G. T.; Prins, W. *Macromolecules* **1974**, *7*, 527.
(34) Carslaw, H. S.; Jaeger, J. C. "Conduction of Heat in Solids", 2nd ed.; Oxford at the Clarendon Press: London, 1959.
(35) Huston, E. L.; Cahn, J. W.; Hilliard, J. E. *Acta Metall.* **1966**, *14*, 1053.
(36) Debye, P. *J. Chem. Phys.* **1959**, *34*, 680.
(37) Reddy, J. N.; Rasmussen, M. L. "Advanced Engineering Analysis"; Wiley: New York, 1982.

Preliminary Study of the Kinetics of Phase Separation in High Molecular Weight Poly(methyl methacrylate)/Solution-Chlorinated Polyethylene Blends

R. G. Hill, P. E. Tomlins,* and J. S. Higgins

Department of Chemical Engineering and Chemical Technology, Imperial College of Science and Technology, London SW7 2BY, England.

Received February 13, 1985

ABSTRACT: Preliminary results of a study of the kinetics of spinodal decomposition in a high molecular weight blend of poly(methyl methacrylate) with solution-chlorinated polyethylene using small-angle light, X-ray, and neutron scattering are reported. The data are compared with the theoretical predictions of Cahn, Hilliard, and van Aartsen. The phase separation occurs initally on a scale much smaller than previously observed for polymeric systems.

Introduction

Despite an ever increasing interest in the thermodynamics of polymer miscibility, there have been comparatively few studies of the kinetics of phase separation in polymer mixtures.

Several theories exist (Pincus,[1] de Gennes,[2] Binder[3]) that describe the process of phase separation in high molecular weight polymer blends where the molecular weights of the components are above their entanglement values. These theories, although differing in their approaches, predict the wavelength of the dominant concentration fluctuation (λ_m) to be of the same order of magnitude as the radius of gyration (R_g) of the polymer for deep quenches. In contrast van Aartsen,[4] using Cahn–Hilliard[5–7] and Flory–Huggins[8,9] theory, predicts that this wavelength will be much larger than R_g and lie in the micron range. λ_m is defined by van Aartsen as

$$\lambda_m = 2\pi l\left[3\left(\frac{T}{T_s} - 1\right)\right]^{-1/2} \quad (1)$$

where l is the Debye[10] range of molecular interaction and T_s and T are the temperature of the spinodal and sample, respectively. This equation differs from the one given by

0024-9297/85/2218-2555$01.50/0

van Aartsen in the term $(T/T_s - 1)$, which has been redefined for a system possessing a lower critical solution temperature by Kwei et al.[11] Debye suggests that l should be equal to the R_g of the polymer, so for a polymer with an R_g of 100 Å at a temperature near the spinodal λ_m would be ca. 1 μm.

To compare these predictions with experimental data the initial correlation lengths should be measured as a function of molecular weight for blends containing monodisperse polymers. In this preliminary study such samples were not available, and the data analysis is initially carried out according to the Cahn–Hilliard theory only.

Cahn[12] described the free energy difference between a homogeneous solution and one containing concentration fluctuations as

$$\Delta G = \int \left[\frac{1}{2}\left(\frac{\partial^2 G}{\partial \phi^2}\right)(\phi - \phi_0)^2 + K(\nabla\phi)^2 \right] dV \quad (2)$$

where ϕ is a local concentration and ϕ_0 the average concentration. $K(\nabla\phi)^2$ is a contribution to the free energy from material located in concentration gradients. It is convenient to analyze the concentration fluctuations in terms of their Fourier components. The contribution to the free energy of the system from a particular component β is then given by

$$G_\beta = \tfrac{1}{4}VA^2[(\partial^2 G/\partial\phi^2) + 2K\beta^2] \quad (3)$$

where V is a volume of solution and A and K are the respective Fourier and gradient energy coefficients. $\beta = 2\pi/\lambda$ where λ is a wavelength. From this expression it can be seen that only those wavelengths with a sufficiently large value (or small wavenumber β less than some critical value β_c) will continue to grow. This critical wavenumber β_c is given by the value where G_β changes sign.

$$\beta_c = [(-\partial^2 G/\partial\phi^2)/2K]^{1/2} \quad (4)$$

Consideration of the variational derivative of ΔG in eq 1 gives the change in concentration as a function of time during a spinodal process as

$$\frac{d\phi}{dt} = M\frac{\partial^2 G}{\partial\phi^2}\nabla^2\phi - 2MK\nabla^4\phi + \text{nonlinear terms} \quad (5)$$

where M is the diffusional mobility. Solving eq 5, ignoring the nonlinear terms which are unimportant at early times, gives

$$\phi - \phi_0 = \sum_{\text{all }\beta} \exp[R(\beta)t][A(\beta)\cos(\beta\cdot\mathbf{r}) + B(\beta)\sin(\beta\cdot\mathbf{r})] \quad (6)$$

A and B are the Fourier coefficients of a component with wavenumber β. $R(\beta)$ is the rate at which the amplitude of β increases and is defined as

$$R(\beta) = -M(\partial^2 G/\partial\phi^2)\beta^2 - 2MK\beta^4 \quad (7)$$

The growth rate $R(\beta)$ shows a rather sharp maximum at

$$\beta_m = \tfrac{1}{2}[-(\partial^2 G/\partial\phi^2)/K]^{1/2} \quad (8)$$

i.e., one particular concentration fluctuation wavelength becomes dominant within the system. In a scattering experiment this situation is seen as a well-defined peak at wavevector Q_m where

$$Q_m = 4\pi\sin\theta/\lambda \quad (9)$$

λ being the wavelength of the incident radiation and θ half the scattering angle. (Substituting Bragg's law ($\lambda = 2d\sin\theta$) into eq 9, we obtain $Q = 2\pi/d$ where d corresponds to a correlation length λ_m, hence $\beta_m = Q_m$.)

The analogy between eq 5 and a conventional diffusion expression, where $d\phi/dt = D\nabla^2\phi$, allows us to obtain a Cahn–Hilliard diffusion coefficient $\bar{D}$ where

$$\bar{D} = M(\partial^2 G/\partial\phi^2) \quad (10)$$

$\bar{D}$ can be calculated from the growth rate of the maximum β_m. Combining eq 7 and 8 gives

$$R(\beta_m) = -\tfrac{1}{2}M\beta^2{}_m(\partial^2 G/\partial\phi^2) \quad (11)$$

and hence

$$\bar{D} = -2R(\beta_m)/\beta_m{}^2 \quad (12)$$

Rundman[13] has shown that the scattered intensity of the most rapidly growing wavevector (Q_m) of a metallic alloy system undergoing spinodal decomposition is given by

$$I(Q_m) \propto \exp[2R(Q_m)t] \quad (13)$$

Thus at early times where the nonlinear terms are unimportant, spinodal decomposition is characterized by the exponential growth of a single scattering peak at fixed Q. Such behavior has recently been observed by small-angle light scattering (SALS) in high molecular weight blends of polystyrene/poly(vinyl methyl ether) (PS/PVME)[14-17] and in an oligomeric system of PS/polybutadiene (PS/PB).[18]

This paper reports an investigation into spinodal decomposition in a blend of solution-chlorinated polyethylene/poly(methyl methacrylate) (SCPE/PMMA). In contrast to suspension-chlorinated polyethylene the SCPE is a totally amorphous randomly chlorinated analogue of poly(vinyl chloride). Chai et al.[19] have studied the thermodynamics of this blend and modeled the phase boundary using the Flory equation of state[20,21] approach. Heat of mixing measurements made by Chai et al. on a model system of chlorinated octadecane and oligomeric PMMA show the enthalpy of mixing to be negative. This is believed to result from a weak hydrogen bond formed between hydrogen atoms in the octadecane and the carbonyl group of the PMMA. These hydrogen bonds are also thought to occur in the polymeric blend.

Contrary to Chai's[22] claim that blends of this system containing SCPE with more than 62% (w/w) chlorine would be totally compatible, we have found evidence for a miscibility window in the phase diagram. SCPE with a chlorine content of 65% is fully miscible with PMMA but SCPE's with chlorine contents of 67% and 72% (w/w) show only partial compatibility.

Experimental Section

The PMMA sample ($M_w = 8.38 \times 10^4$, $M_w/M_n = 2.42$) was obtained from Polysciences Ltd. The SCPE sample ($M_w = 8.08 \times 10^5$, $M_w/M_n = 6.45$) was prepared in the laboratory by passing chlorine through a solution of polyethylene in chlorobenzene at 140 °C for several hours.[23] The chlorine content of the SCPE was found by elemental analysis to be 67.5% w/w. Chai et al.[24] have studied the distribution of chlorine atoms in SCPE by NMR spectroscopy and shown for samples containing more than 50% w/w chlorine that they are randomly located along the polyethylene chains. Fully deuterated PMMA was synthesized in our laboratory with 2,2′-azobis(isobutyronitrile) as the initiator, and molecular weight fractionated by using acetone/methanol/water mixtures. The fourth fraction ($M_w = 9.61 \times 10^4$, $M_w/M_n = 1.30$) was used in this study.

Thin films of the blends were made by evaporating solutions containing known weights of PMMA and SCPE dissolved in chlorobenzene to dryness. The films were then placed under vacuum at 80 °C for a period of at least 7 days to ensure that all traces of the solvent were removed. Typical film thicknesses were 0.1–0.2 mm.

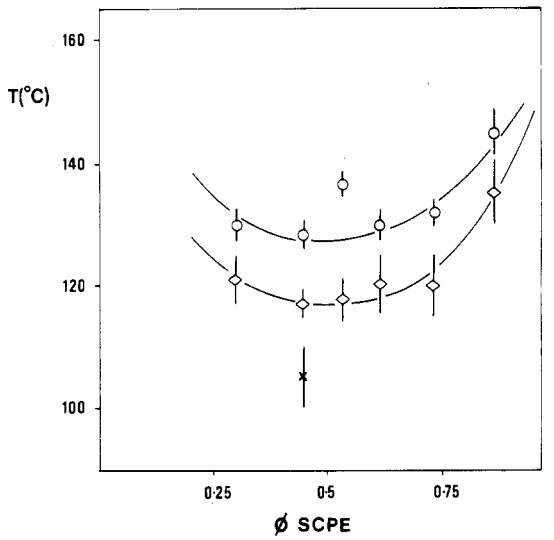

Figure 1. Phase boundary for the system SCPE/PMMA as determined by SALS (○) and SAXS (◇). Point **X** contained deuterated PMMA, and its position was found by SAXS.

Light-scattering experiments to determine the position of the phase boundary were carried out by using a purpose-built apparatus.[25]

SAXS experiments on hydrogenous samples were performed by using the small-angle camera (Station 7) on the high-flux synchroton radiation source (Daresbury, England). The scattered intensity was recorded by a single wire proportional counter at a distance of 2.17 m from the sample. The X-ray wavelength was 1.608 Å. Corrections were made for the detector response but not for slit smearing, since the beam is a fairly good approximation to a point source in the meridianal direction. Parasitic scattering near the beam stop was removed by subtracting the spectrum of a non phase-separated sample of equivalent thickness.

Small-angle neutron-scattering (SANS) experiments on samples containing deuterated PMMA were performed on the D11 spectrometer[26] at the Institut Laue-Langevin (Grenoble, France). A sample–detector distance of 10.6 m was used with neutrons of wavelength 8.08 Å ($\Delta\lambda/\lambda = 8\%$). Corrections were made for the detector response by using the incoherent scattering from water.

The use of high-flux sources opened the possibility of real time experiments. These were performed by monitoring the scattered intensity as a function of time after a thin polymer film contained within a brass sample holder was plunged into a preheated temperature controlled block. Spectra were recorded for periods of 10–20 s with no lag time between successive measurements. Calibration showed the temperature jump to be effectively complete within 5 s.

Results and Discussion

The phase boundary determined by light-scattering measurements on hydrogenous samples is shown in Figure 1. Cloud points were difficult to locate by this technique, as plots of the scattered intensity as a function of temperature did not show a sharp transition even with low heating rates of 0.1 °C min^{-1}.

A series of samples were investigated by using SAXS and shown to be homogeneous prior to any heat treatment. However, at temperatures close to the phase boundary the samples, although optically clear, were found to strongly scatter X-rays. This suggested that phase separation was initially taking place on a much shorter distance scale than could be observed by light scattering. The phase boundary was therefore redetermined by this technique and is also shown in Figure 1.

Also shown in Figure 1 is one point on the phase boundary for deuterated PMMA by SAXS. The slightly lower temperature of phase separation could be a result of the much narrower molecular weight distribution of the deuterated material or, more likely, a slight difference in the stereochemistry of the polymer backbone.

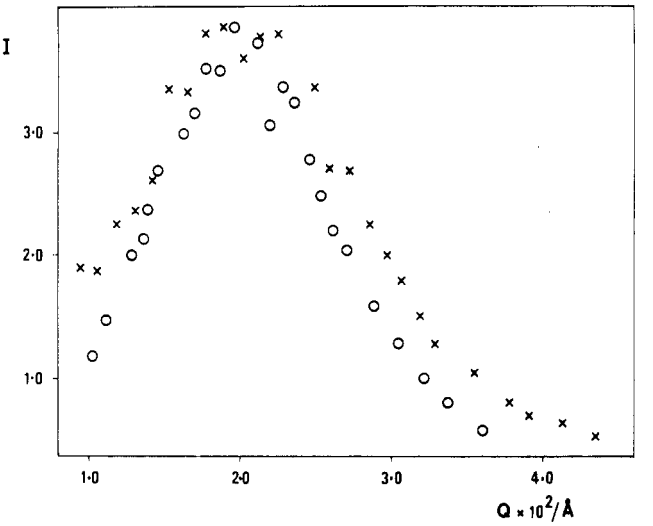

Figure 2. Plots of intensity against Q for a hydrogenous sample that was quenched after being at 150 °C for 30 s, as observed by SAXS (○) and SANS (**X**).

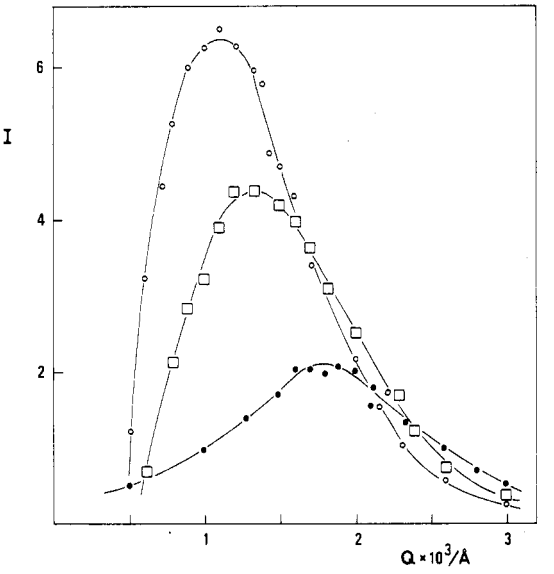

Figure 3. SAXS data showing $I(Q)$ as a function of time for a hydrogenous sample containing 55% SCPE at 117 °C: (•) 50 s, (□) 100 s, (○) 170 s.

Since the initial correlation length λ_m was found to be outside the range of light scattering, studies of the kinetics of phase separation were limited to SANS and SAXS experiments. The results obtained by these techniques are compared in Figure 2, which shows $I(Q)$ for a quenched hydrogenous sample. At high Q the agreement between the two data sets is not particularly good. This discrepancy almost certainly arises because of the practical difficulty of uniformly heating the sample for a given time such that all regions will have phase-separated to the same extent. Such local differences become important when one considers the small size of the X-ray beam in contrast to the 1-cm diameter neutron beam.

The SAXS data shown in Figure 3 illustrates the development with time of the scattered intensity as a function of Q for a sample containing 55% SCPE. Plots of λ_m derived from the peak positions against log time are shown in Figure 4. λ_m during the early stages should remain fixed; clearly the plots in Figure 4 do not obey this criterion, suggesting that the early stages are complete within a very short period of time. This behavior is to be expected

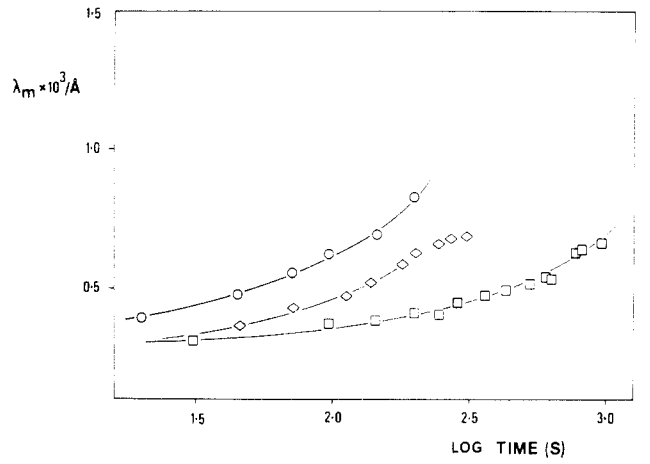

Figure 4. Correlation length λ_m as a function of time for samples containing 55% SCPE at 147 °C (○), 140 °C (◇), and 130 °C (□) (SAXS data).

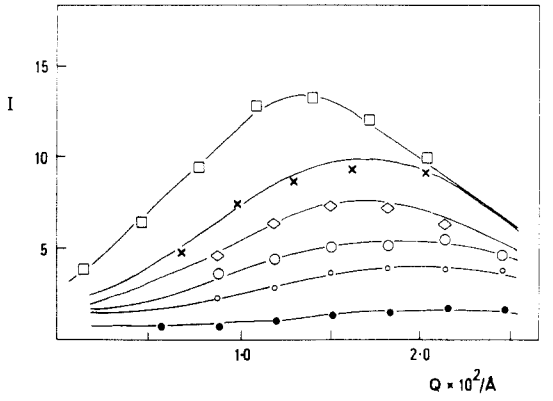

Figure 5. SANS data showing $I(Q)$ as a function of time for a sample containing deuterated PMMA and 55% SCPE at 117 °C: (•) 30 s, (○) 80 s, (○) 110 s, (◇) 150 s, (x) 200 s, (□) 290 s. (Most of the data points have been omitted for clarity.)

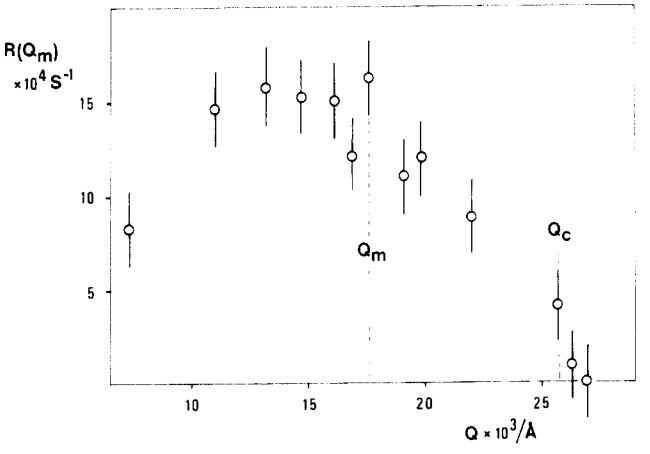

Figure 6. Cahn–Hilliard growth rate $R(Q)$ as a function of wavevector for a sample containing 55% SCPE and deuterated PMMA at 113 °C (SANS data).

for any system where the initial λ_m is small, since the chains need only diffuse a short distance (~300 Å) in order to achieve the equilibrium concentrations defined by the coexistence curve. Not all high molecular weight blends phase-separate with such small initial correlation lengths; for example, Hashimoto et al.[14] have measured λ_m as ca. 7000 Å in a blend of PS/PVME and shown the early stages to persist for several minutes.

Figure 5 shows $I(Q)$ measured by SANS as a function of time for a blend containing 55% SCPE with deuterated

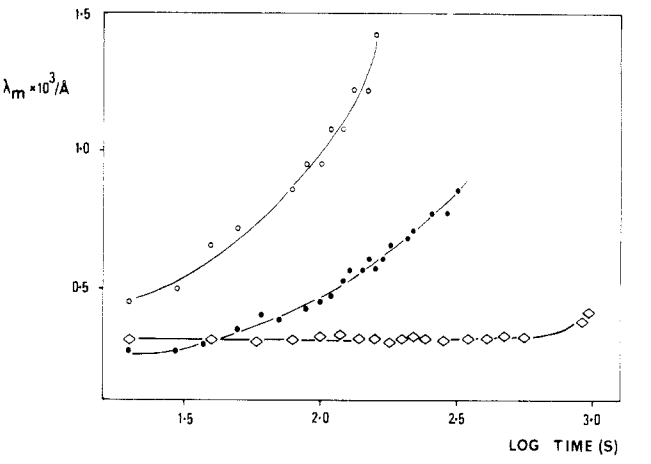

Figure 7. Development of the correlation length λ_m as a function of time for samples containing deuterated PMMA and 55% SCPE (SANS data): (○) 150 °C, (•) 131 °C, (◇) 113 °C.

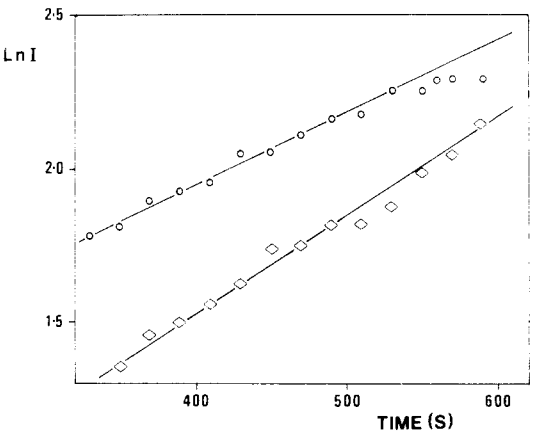

Figure 8. SANS data showing ln I as a function of time for a sample containing deuterated PMMA and 55% SCPE at 113 °C measured at Q vectors of 1.98×10^{-2} Å^{-1} (○) and 2.7×10^{-2} Å^{-1} (◇).

Table I
Values of $R(Q_m)$, $\bar{D}$, and Q_m for a Sample Containing 55% SCPE with Deuterated PMMA

temp, °C	$R(Q_m) \times 10^{-3}$	$Q_m \times 10^{-2}$ Å^{-1}	$\bar{D} \times 10^{-15}$ cm^2 s^{-1}
113	16.8	1.76	−1.1
117	32.3	2.20	−13.3

PMMA at 117 °C. The diffuse nature of the peak at early times makes it difficult to determine the position of maximum intensity and hence to decide whether or not the data can be analyzed in terms of the Cahn–Hilliard theory. This difficulty can be overcome by plotting the growth rate $R(Q)$ as a function of wavevector, as shown in Figure 6. The Q vector at which the maximum growth rate $R(Q_m)$ occurs corresponds to the position of λ_m.

Figure 7 shows the correlation length λ_m as a function of time. Clearly, at 150 °C phase separation has progressed beyond the early stages. Comparison of the data at 113 °C with that obtained at 131 °C suggests that the initial correlation length increases with decreasing temperature. This is in agreement with eq 1, which predicts that the initial wavelength of the composition fluctuations will tend to infinity as the spinodal is approached. Such an observation provides some evidence against phase separation proceeding from any structure that may exist within the blend.

At 113 °C, λ_m remains constant as a function of time for approximately 600 s (Figure 7). During this period the

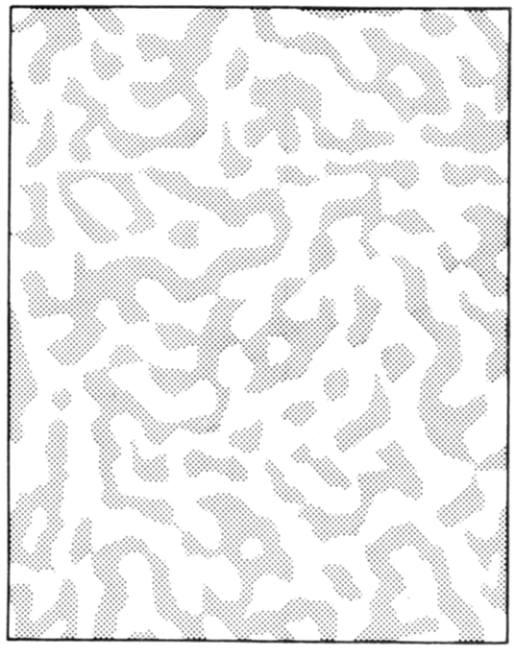

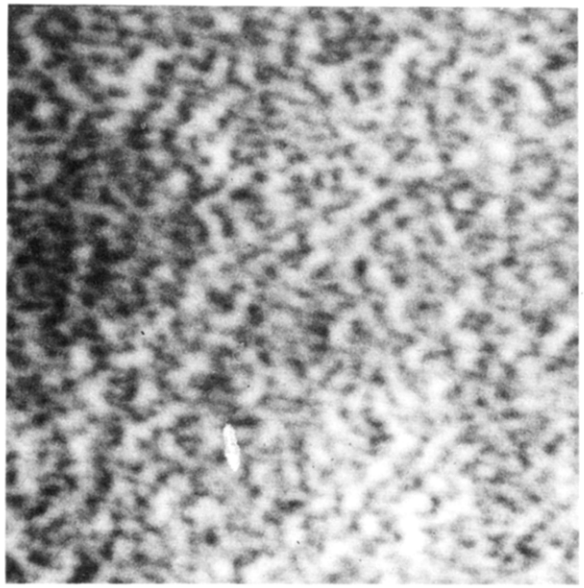

Figure 9. (top) Computer simulation of the interconnected structure characteristic of spinodal decomposition, redrawn from Cahn.[20] (bottom) Transmission electron micrograph from a sample containing 55% SCPE with deuterated PMMA showing an interconnected structure; note the similarity with (a).

scattered intensity at λ_m increases exponentially, as shown in Figure 8.

Snyder et al.[15-17] have also demonstrated that λ_m remains approximately constant while the scattered intensity increases exponentially in their SALS studies on PS/PVME mixtures. At later times the intensity stops growing exponentially and the correlation length starts to increase. Theoretically this would correspond to the nonlinear terms neglected by Cahn–Hilliard becoming important.

The values of $R(Q_m)$, $\bar{D}$, and Q_m are listed in Table I. The magnitude of $\bar{D}$ is much less than values reported for other polymer blends such as PS/PVME where $\bar{D}$ is typically between 10^{-10} and 10^{-13} cm^2 s^{-1}. This result is quite acceptable, considering the high molecular weights of the components and the close proximity of the measurement temperature to the blend T_g, which calculated from the Flory–Fox equation would be 111 °C.

A series of hydrogeneous samples containing 55% SCPE (w/w) were heated to 150 °C and then quenched after remaining at that temperature for a known period of time. Some of these samples when examined by transmission electron microscopy (TEM) were found to possess an interconnected morphology which is consistent with the theory of spinodal decomposition (Figure 9). However, it is known from the SAXS and SANS data that these samples are no longer in the early stages as defined by the Cahn–Hilliard theory. Samples in the early stages were found to be featureless when investigated by TEM. This is no doubt due to the poor contrast between the phases during this period.

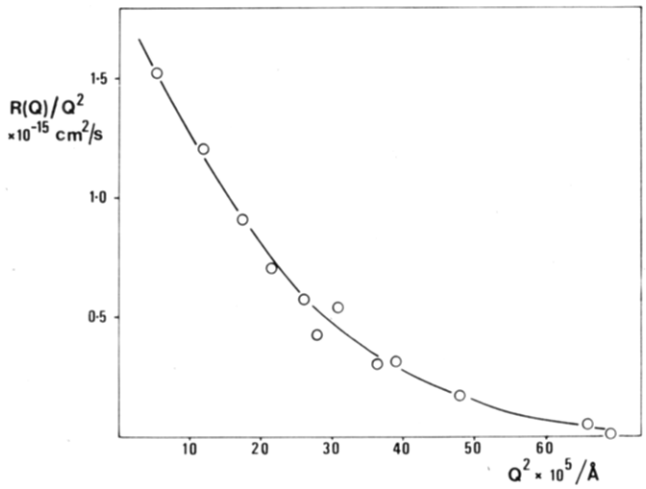

Figure 10. $R(Q)/Q^2$ against Q^2. Cahn–Hilliard model predicts that this plot should be linear.

Experimental studies on metallic alloys have shown that parts of the Cahn–Hilliard model required further modifications. The relationship $Q_c/Q_m = 2^{1/2}$ (eq 4 and 8) is not generally found experimentally; most studies report higher values.[27,28] Park et al.,[29] using Cook's modified theory[30] which takes into account the effects of microconcentration fluctuations, have shown that Q_c/Q_m will only fall to $2^{1/2}$ at absolute zero. Although quantitatively correct, the experimental values are in poor agreement with values calculated by Park et al. Our value of 1.51, although inconsistent with Cahn–Hilliard theory, is comparable with those found in the small molecule systems. A second deficiency of the Cahn–Hilliard theory is shown in Figure 10. Equation 7 can be rearranged to give

$$R(\beta) = -M\beta^2[(\partial^2 G/\partial\phi^2) - 2K\beta^2] \qquad (14)$$

Clearly this expression predicts a linear relationship between $R(Q)/Q^2$ and Q^2 which is not shown in the figure. Given that the initial correlation length is comparable to the radius of gyration, the curvature of this plot could be explained by a wavevector-dependent diffusion coefficient, as proposed by Pincus.[1] However, plots of $R(Q)/Q^2$ as a function of Q^2 show curvature in metallic alloys,[26] oligomeric mixtures of polystyrene with polybutadiene,[18] and a mixture of PS/PVME[15] (but not in another[14]). In these systems the curvature cannot be explained by a wavevector-dependent diffusion coefficient because for all of them (except metallic alloys) the initial correlation length is much larger than that predicted by Pincus. It has been suggested that inclusion of the nonlinear terms in the Cahn–Hilliard theory might improve this situation. However, if this were the case, a nonlinear relationship between ln I and time contrary to eq 8 might occur at high Q vectors where the nonlinear terms become more important. Such a hypothesis is difficult to test because of poor statistics. A second explanation first proposed by

Erb[31] and Hilliard[32] for these deficiencies is that regular solution theory on which the Cahn–Hilliard model is based may not fully describe the behavior of either small molecule or polymer systems.

The question of why this high molecular weight system should phase-separate on a much smaller scale than the high molecular weight mixtures of PS/PVME remains unanswered. Until we have investigated other systems showing similar behavior (as yet, no other is known), it is not possible to eliminate an explanation in terms of some unique properties of this blend. However, we can at this stage rule out a hypothesis based on "blockiness" in the SCPE.[24] We are continuing this study using monodisperse fractions of both polymers in order to determine the effects of molecular weight on the initial phase size and hence to test the entanglement theory of Pincus.

Acknowledgment. The financial support of the Science and Engineering Research Council is gratefully acknowledged. We would also like to thank the following: Dr. H. L. Snyder for stimulating discussions during the course of this work and Drs. A. Wright, R. Ghosh, and C. Nave for their help with the SANS and SAXS experiments. We also thank our colleagues at Unilever Research (Colworth House) for allowing us access to their X-ray apparatus.

Registry No. PMMA (homopolymer), 9011-14-7; deuterated PMMA (homopolymer), 98821-48-8.

References and Notes

(1) Pincus, P. *J. Chem. Phys.* **1981**, *75*, 1996.
(2) de Gennes, P. G. *Macromolecules* **1979**, *9*, 587.
(3) Binder, K. *J. Chem. Phys.* **1983**, *79*, 6387.
(4) van Aartsen, J. J. *Eur. Polym. J.* **1970**, *6*, 919.
(5) Cahn, J. W.; Hilliard, J. E. *J. Chem. Phys.* **1958**, *28*, 258.
(6) Cahn, J. W.; Hilliard, J. E. *J. Chem. Phys.* **1959**, *31*, 688.
(7) Cahn, J. W. *Acta Metall.* **1961**, *9*, 795.
(8) Flory, P. J. *J. Chem. Phys.* **1940**, *10*, 51.
(9) Huggins, M. L. *Ann. N. Y. Acad. Sci.* **1942**, *431*.
(10) Debye, P. *J. Chem. Phys.* **1959**, *31*, 680.
(11) Nishi, T.; Wang, T. T.; Kwei, T. K. *Macromolecules* **1975**, *8*, 277.
(12) Cahn, J. W. *J. Chem. Phys.* **1964**, *42*, 93.
(13) Rundman, K. B.; Hilliard, J. E. *Acta Metall.* **1967**, *15*, 1025.
(14) Hashimoto, T.; Kumaki, J.; Kawai, H. *Macromolecules* **1983**, *16*, 641.
(15) Snyder, H. L.; Meakin, P.; Reich, S. *Macromolecules* **1983**, *16*, 757.
(16) Snyder, H. L. *J. Chem. Phys.* **1983**, *78*, 3334.
(17) Snyder, H. L.; Meakin, P. *Polym. Prepr. (Am. Chem. Soc., Div. Polym. Chem.)* **1983**, *24*, 411.
(18) Hill, R. G.; Tomlins, P. E.; Higgins, J. S. *Polymer*, in press.
(19) Chai, Z.; Ruona, S.; Walsh, D. J.; Higgins, J. S. *Polymer* **1983**, *24*, 263.
(20) Flory, P. J.; Orwoll, R. A.; Virug, A. *J. Am. Chem. Soc.* **1964**, *86*, 3507.
(21) Eichinger, B. E.; Flory, P. J. *Trans. Faraday Soc.* **1968**, *64*, 2035.
(22) Chai, Z., personal communication.
(23) Chai, Z. Ph.D. Thesis, Imperial College, 1982, London.
(24) Chai, Z.; Lianghe, S.; Sheppard, R. N. *Polymer* **1984**, *25*, 364.
(25) Chong, C. L. Ph.D. Thesis, Imperial College, 1981, London.
(26) Ibel, K. *J. Appl. Cryst.* **1976**, *9*, 296.
(27) Agarwal, S.; Herman, H. *Scr. Metall.* **1973**, *7*, 503.
(28) Acuna, R.; Bongiglioni, A. *Acta Metall.* **1974**, *22*, 399.
(29) Park, M. W.; Cooper, A. R.; Huer, A. H. *Scr. Metall.* **1975**, *9*, 32–330.
(30) Cook, H. E. *Acta Metall.* **1970**, *18*, 297.
(31) Erb, D. Ph.D. Thesis, Northwestern University, Evanston, IL, 1969.
(32) Hilliard, J. E. "Phase Transformations"; Aaronson, H. I., Ed.; American Society for Metals: Metals Park, OH, 1970; p 497.

Molecular Characterization of Poly(2-methyl-1,3-pentadiene) and Its Hydrogenated Derivative, Atactic Polypropylene

Xu Zhongde,[1a] Jimmy Mays,[1b] Chen Xuexin,[1c] and Nikos Hadjichristidis[1d]

The Institute of Polymer Science, University of Akron, Akron, Ohio 44325

F. C. Schilling and H. E. Bair

AT&T Bell Laboratories, Murray Hill, New Jersey 07974

Dale S. Pearson and Lewis J. Fetters*

Exxon Research and Engineering Company, Corporate Research—Science Laboratories, Clinton Township, Annandale, New Jersey 08801. *Received April 22, 1985*

ABSTRACT: The anionic polymerization of (*E*)-2-methyl-1,3-pentadiene leads to near-monodisperse poly(1,3-dimethyl-1-butenylene) (PDMB). The hydrogenation of PDMB yields atactic polypropylene (PP). We report the complete characterization of the microstructure and thermal properties of these two polymers. The carbon-13 NMR spectral analysis reveals that PP is a head-to-tail, ideal-Bernoullian (P_m = 0.502) material. The characteristic ratios for the two polymers were determined under Θ conditions, and, for the case of PP, good agreement is found with the value calculated by Suter and Flory using the five-state rotational isomeric state (RIS) model. The glass transition temperature for the ideal-Bernoullian PP was found to be −2.5 °C, which is about 10 °C higher than values previously reported for non-Bernoullian atactic PP. The conversion of PDMB to atactic PP results in an increase in flexible bonds from three to four along the backbone and in a 28% increase (0.100–0.128 cal g^{-1} $°C^{-1}$) in the change of heat capacity at T_g between the glassy and liquid states of the respective polymers. Comparisons with previous studies on the thermal properties of PP are discussed.

Introduction

The anionic polymerization of (*E*)-2-methyl-1,3-pentadiene initiated by *n*-butyllithium in benzene solution was first quantitatively examined by Cuzin, Chauvin, and Lefebvre.[2] Their microstructure analysis of poly(2-methyl-1,3-pentadiene), IUPAC name poly(1,3-dimethyl-1-butenylene) (PDMB), demonstrated that the reaction exclusively yields the 1,4-configuration where the cis:trans ratio was approximately 60:40. Later studies by Morton and Falvo[3] showed that monomer incorporation takes place exclusively via 4,1-addition, i.e., where the methyl groups are on the β and δ carbons of the terminal unit. The active center was defined as essentially covalent, an assessment in agreement with current understanding[4] regarding alkyl and primary allylic carbon–lithium bonds in nonpolar solvents. The microstructure analysis of Morton and

0024-9297/85/2218-2560$01.50/0